Dynamics of a model for the degradation mechanism of aggregated α-synuclein in Parkinson's disease

Enrique Almazán Sánchez

January 10, 2024

1. Introduction.

The prevalence of Parkinson's disease (PD) is remarkable as the second most common neurodegenerative disease, characterized by the loss of dopaminergic neurons and the formation of Lewy bodies due to abnormal α-synuclein (αSyn) accumulation. The detrimental impact of increased αSyn levels on mitochondrial function and the generation of reactive oxygen species (ROS) is discussed, linking it to the damage of dopaminergic neurons in PD.

The role of autophagy-lysosome pathway (ALP) in degrading αSyn is emphasized for maintaining homeostasis in PD pathology, with a focus on the need to integrate ALP clearance mechanisms into existing models. Also, the mammalian target of rapamycin (mTOR) is introduced as a central regulator of ALP and a potential therapeutic target for PD.

The complex interplay between mTOR, ALP, and αSyn is discussed, acknowledging mTOR's role in regulating ALP and the potential significance of targeting this crosstalk for PD treatment. The connection between αSyn aggregation and endoplasmic reticulum (ER) stress responses, clarifies the dual role of autophagy in maintaining neuro-homeostasis under tolerable stress and switching to apoptosis under excessive stress levels.

Additionally, the existence of healthy, critical, and disease states in PD pathology, considering the tri-stability of αSyn is studied, focusing on the key molecules Beclin1 and mTOR in ALP, studying their roles under three different stresses through codimension-1 bifurcation diagrams. The impact of ALP-dependent degradation rates on tri-stability under various stresses is surveyed, emphasizing the bistable state switch from irreversible to reversible under internal and external oxidative stresses. The robustness of the tri-stable state concerning mTOR-associated regulatory mechanisms is also explored. Overall, the findings provide new insights into the complex tri-stability dynamics as a key regulatory mechanism where mTOR-mediated ALP degrades αSyn in PD.

Hence, a mathematical model focusing on mTOR-mediated ALP as a major protein clearance mechanism for degrading aggregated αSyn is presented. Two key points are outlined: the activation of ERS, ALP, and Caspases-dependent apoptosis (blue) triggered by ROS-induced αSyn aggregation (orange), and the control of ALP (green) degradation of αSyn by mTOR crosstalk, shown in the figures below. The non-linear dynamic analysis is emphasized for understanding the protein concentration tendencies crucial in disease emergence.

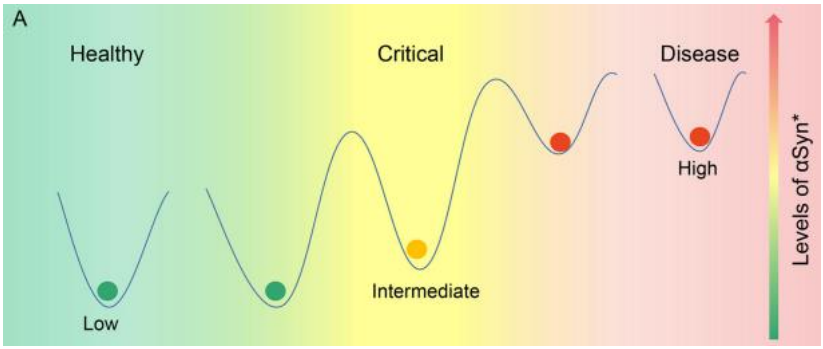

Figure 1: Three different states, low, intermediate, and high steady states parallel to the healthy, critical, and disease states, respectively, according to the levels of αSyn.

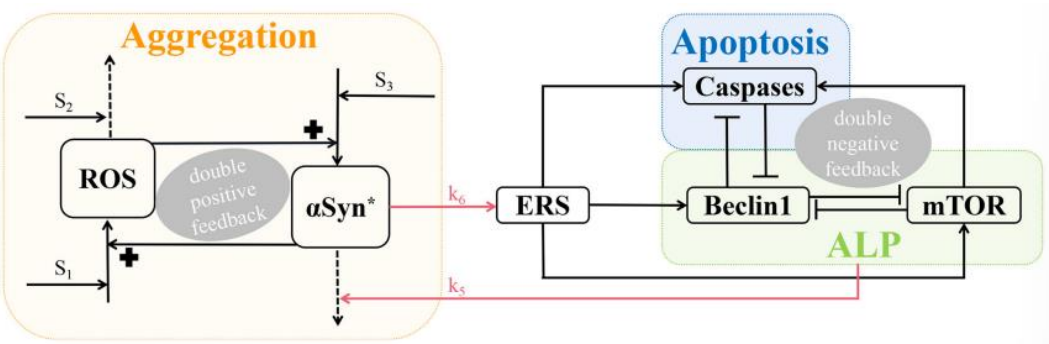

Figure 2: A three-module model network characterizing aggregation, ALP, and apoptosis. The promotion, degradation, and inhibition are denoted by solid lines with arrowheads, dotted lines with arrowheads, and blocked end lines, respectively.

As seen above, aggregation involves a positive feedback loop between misfolded αSyn and ROS under three stresses (S1, S2, and S3). S1, induced by internal or external oxidative stress, promotes ROS, while S2, associated with age-related anti-oxidative mechanisms, degrades ROS. S3, characterized by damaged protein mechanisms, facilitates αSyn formation.

Endoplasmic reticulum stress, activated by αSyn, triggers Beclin1-dependent autophagy via ALP, Caspases-dependent apoptosis, and mTOR. αSyn aggregation through ALP involves both mTOR signalling and Beclin1-associated pathways, forming three double-negative feedback loops. These loops inhibit Beclin1-Caspases, Beclin1-mTOR, and Beclin1-Caspases-mTOR interactions when activated mTOR promotes Caspases. The model provides insights into the intricate dynamics of αSyn∗ ROS, and their interplay with autophagy and apoptosis, offering a comprehensive view of the regulatory mechanisms involved in Parkinson's disease pathology.

1.1. Dynamic Equations.

The formulation of the model involves a system of coupled non-linear ordinary differential equations (ODEs). This system comprises six components, representing the concentrations of [ROS], [αSyn], [ERS], [mTOR], [Beclin1], and [Caspases].

The double-positive feedback loops between [ROS] and [αSyn] are described in the following two equations. For the former, the first term represents [ROS] generated by the background synthesis, stimuli S_1, and [αSyn∗], while the second represents [ROS] degraded by stimuli S_2.

$$\frac{d[ROS]}{dt} = k_1\left[1 + S_1 + d_{\alpha\text{Syn}}\left(\frac{\left(\frac{[\alpha\text{Syn}]}{k_{\alpha\text{Syn}}}\right)^4}{1+\left(\frac{[\alpha\text{Syn}]}{k_{\alpha\text{Syn}}}\right)^4}\right)\right] - k_2 \cdot [ROS] \cdot S_2$$

The next equation represents the dynamics of aggregated αSyn, including [ROS] which promotes the generation of αSyn within the first term, and the basal and Beclin-1-dependent removal within the second term.

$$\frac{d[\alpha\text{Syn}]}{dt} = k_3 \cdot [ROS] \cdot S_3 - k_4 \cdot [\alpha\text{Syn}] \cdot k_5 \cdot ([Beclin1] \cdot [mTOR])$$

For the dynamics of the endoplasmic reticulum stress sensor (ERS) a first term corresponds to [ROS]-dependent and basal activation of [ERS], while the second term corresponds to the basal inactivation of [ERS].

$$\frac{d[\text{ERS}]}{dt} = k_6 \cdot [\alpha\text{Syn}] \cdot k_7 \cdot (ERST - [ERS]) - k_8 \cdot [ERS]$$

Regarding the mammalian target of rapamycin (mTOR), its dynamics involve the basal and [ERS]-dependent activation represented by the first term, as well as the basal and [Beclin1]-dependent inactivation represented by the second term.

$$\frac{d[\text{mTOR}]}{dt} = (k_9 + k_{10} \cdot [ERS]) \cdot (mTORT - [mTOR]) - (k_{11} + k_{12} \cdot [Beclin1]) \cdot [mTOR]$$

Finally, the double negative feedback loops between [Beclin1] and [Caspases] is described in the following equations. The fifth equation accounts for the dynamics of [Caspases] with two terms, the basal and [ERS]-dependent activation and the basal and [Beclin1]- dependent inactivation.

$$\frac{d[\text{Beclin1}]}{dt} = \frac{(k_{13} + k_{14} \cdot [ERS]) \cdot (Beclin1T - [Beclin1])}{(J_{be} + Beclin1T - [Beclin1])} - \frac{(k_{15} + k_{16} \cdot [Caspases] + k_{17} \cdot [mTOR]) \cdot [Beclin1]}{(J_{be} + [Beclin1])}$$

$$\frac{d[\text{Caspases}]}{dt} = \frac{(k_{18} + k_{19} \cdot [ERS] + k_{20} \cdot [mTOR]) \cdot (CaspasesT - [Caspases])}{(J_{ca} + CaspasesT - [Caspases])}$$

All the constants found in the previous system of equations are well defined in the original article.

2. Results.

2.1. Bifurcations analysis under the three stresses.

The impact of three different stresses (S1, S2, and S3) on the activation of αSyn, Caspases, and Beclin1 in a positive-feedback loop with ROS is first tested. Bifurcation diagrams were created to illustrate the concentration changes in αSyn, Caspases, and Beclin1 under these stresses. Multiple stable and unstable branches were identified, leading to tri-stability, bistability, or monostability for each stress. Tri-stability dominated for S1 in a specific range, while S2 and S3 exhibited different dominant ranges.

In addition, the reversibility of state transitions for the stresses was also explored. S2 and S3 showed reversible switching between stable states, impacting αSyn concentrations, whereas S1 had irreversible transitions due to fold bifurcation points. The results emphasize the dynamic nature of the three stable states and their biological significance.

Finally, it has been shown that the model's non-negative stresses hold biological significance, influencing reversible or irreversible switching between stable states, thereby impacting αSyn concentrations.

2.2. Tri-stability initiated from different values of the [αSyn] concentration.

The examination of time series data unveils biological insights into the effects of different initial values of [αSyn]. Small values result in low concentrations, accompanied by elevated [Beclin1] and diminished [Caspases], indicating a health state where Beclin1-induced autophagy efficiently degrades most [αSyn]. Intermediate values lead to moderate concentrations, low [Beclin1], and intermediate [Caspases], suggesting a critical state with relatively low [αSyn], dominated by apoptosis. In contrast, large values result in high concentrations, elevated [Caspases], and intermediate [Beclin1], indicating a disease state attributed to the high [αSyn] concentration. These findings offer valuable biological context to the dynamic interactions among αSyn, Caspases, and Beclin1, revealing their implications for different physiological states.

2.3. Tri-stability under the three stresses controlled by the ALP-dependent degradation rate k_5.

The accumulation of αSyn is subject to degradation by ALP, involving both mTOR-signalling and Beclin1-associated pathways. The model incorporates the ALP-dependent αSyn degradation rate constant, k5, linking two modules through ALP's degradation mechanism. By varying k5, the bifurcation curves of αSyn in response to stress signals S1, S2, and S3 are explored. Different k5 values shift the bifurcation curves, moving left to right for S1 and S3 but in the opposite direction for S2.

Hence, increasing k5 changes irreversibility to reversibility in the bistable switch between middle and upper stable states for S1, facilitating the transition from upper to middle states. Moreover, elevated k5 significantly lowers upper stable states, reducing αSyn levels. This supports the notion that αSyn aggregation can be modulated by k5 through ALP degradation pathways, suggesting that ALP, regulated by mTOR, plays a crucial role in controlling the switch between irreversible and reversible states.

2.4. Regions of tri-stable steady states in codimension-2 bifurcation diagrams.

The parameter k5 plays a crucial role in shaping bifurcation curves and determining transitions between stable steady states. Codimension-2 bifurcation diagrams in (Si, k5)-planes reveal intricate patterns.

On the (S1, k5)-plane, four fold bifurcation curves (f1–f4) and a Hopf bifurcation curve near f3 delineate tri-stable (T, green), bistable (B, pink), and monostable (M, yellow) regions. The number of stable equilibria changes at fold curve f3 due to fold bifurcation and Hopf bifurcation. Similar patterns are observed in (S2, k5)-plane and (S3, k5)-plane, where fold curves f1–f4 and the Hopf curve divide the planes into regions M, B, and T.

The codimension-2 diagrams comprehensively depict multi-stability, emphasizing the dynamics of the tri-stable state (T) and its potential role in transitioning from a healthy to a critical state, avoiding a direct shift to disease. Notably, the tri-stability region for S1 is larger than that for S2 and S3, and the irreversible switch becomes reversible in the tri-stable region for S1 with increasing k5, highlighting the significance of the ALP degradation pathways regulated by k5 in maintaining the tri-stable state under stress S1.

2.5. Fluctuation of the [αSyn] steady-state levels under different initiated condition.

The selection of initial values significantly influences αSyn accumulation and the attainment of different stable states in tri-stability. A comprehensive examination of the impact of different initial conditions on steady-state αSyn levels was conducted for stresses Si (i = 1, 2, 3) and parameter k5. The three initial [αSyn∗] values (0, 2, 10) were assessed, revealing 3D and 2D contour maps. The surfaces represent stable steady states for Si (x-axis) and k5 (y-axis), projected onto (Si, k5) planes.

Increasing initial [αSyn∗] values lead to elevated steady-state levels and a reduction in the regions of lower stable states (blue). Notably, the impact is more pronounced in the (S1, k5)-plane. Also, larger k5 expands regions of lower steady-state levels, potentially reducing [αSyn], particularly with larger k5 and smaller stresses S1 and S3.

Thus, k5 plays a crucial role in regulating αSyn∗ concentration, particularly in the context of stress S1, offering insights for Parkinson's disease prevention and treatment.

2.6. Robustness of tri-stable state to the parameters of mTOR-related regulations.

Finally, an assessment of the robustness of tri-stable regions in the (S1, k5)-plane was conducted by varying key parameters associated with mTOR, specifically the αSyn-dependent rate constant of ERS activation (k6) and the basal rates of mTOR activation (k9) and inactivation (k11).

Codimension-2 bifurcation diagrams were examined as the raw values of k6, k9, and k11 were altered. Increasing k6 shifted fold bifurcation curves f3 and f4 leftward, causing the tri-stable region (T) to shrink while bistable region (B) expanded slightly between f1 and f2. Parameter k9 showed little impact on bifurcation curves or steady-state regions, indicating robust dynamic behaviour to k9 perturbation. Unexpectedly, increasing k11 transformed the tri-stable state into a bistable state, and further changes led to a monostable state.

Therefore, perturbation of parameter k11 had the most significant impact on the dynamic behaviour of the tri-stable state in the (S1, k5)-plane, underscoring the crucial role of mTOR-mediated autophagy in maintaining this system's essential dynamic features.

3. Discussion.

The role of αSyn aggregation in the pathogenesis of PD is defined by the previous explained mathematical model to understand the dynamics of the disease progression. The model suggests that the ALP regulated by the mTOR is a major mechanism for degrading aggregated αSyn.

The concept of tri-stability in PD progression is presented, dividing it into three states: normal, pre-disease (or tipping point), and disease states, captured through codimension-1 bifurcation analysis, with stable states corresponding to healthy, critical, and disease states. Also, the irreversibility of stress S1, linked to mitochondrial dysfunction and increased ROS, contributes to the maintenance of high αSyn concentrations.

Finally, the importance of mTOR-mediated ALP and its clearance mechanisms in regulating αSyn degradation and the robustness of tri-stability under certain parameters is presented. The intermediate state is identified as a critical barrier preventing the direct transition from a lower to an upper steady state, being as an alert for potential PD development.

The model proposes that targeting the critical state in neuron cells and controlling the ALP pathways could be vital for preventing further αSyn aggregation, protect dopaminergic neurons from death. and, consequently, PD. This will aim to bridge experimental and theoretical biology for a more comprehensive understanding of αSyn degradation, potentially leading to novel therapeutic approaches for treating Parkinson's disease through biomathematical modelling.

4. Implementation of the dynamic systems.

In this section, the findings and models presented in the article will be implemented, focusing on two sections of the original article.

- Representation of the six differential equations over time with Matlab.
- Representation of the bifurcation diagrams and analysis of the tri-stability with XPP- AUTO.

To carry out this implementation, collaboration with the authors of the article was established, who kindly shared the original codes in Matlab and XPP-AUTO.

Only the previous sections mentioned were taken into account as trying to reproduce the entire article was non-viable.

4.1. Representation over time through Matlab implementation.

The Matlab code will focus on the graphical representation of each concentration over time. The results obtained by the authors were sought to be reproduced, generating our own Matlab code to compare and validate the outcomes. This process was crucial to ensure accuracy and consistency in implementing the proposed model.

First of all, the author results are shown below given by the Matlab function 'time.m' presented with the project. It is needed to mention that some plots were added in order for the comparison to be consistent.

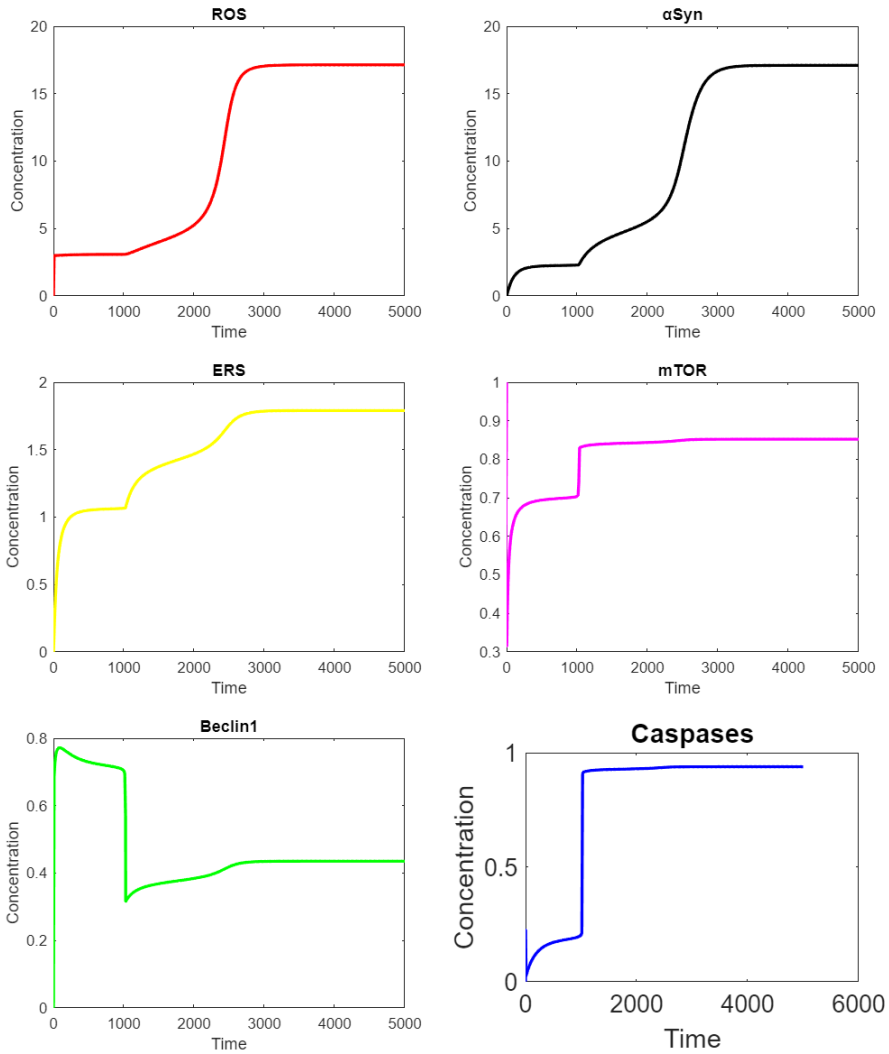

Figure 3: Outputs given by the author code, 'time.m'.

Now the outputs obtained by the code implemented by me are presented.

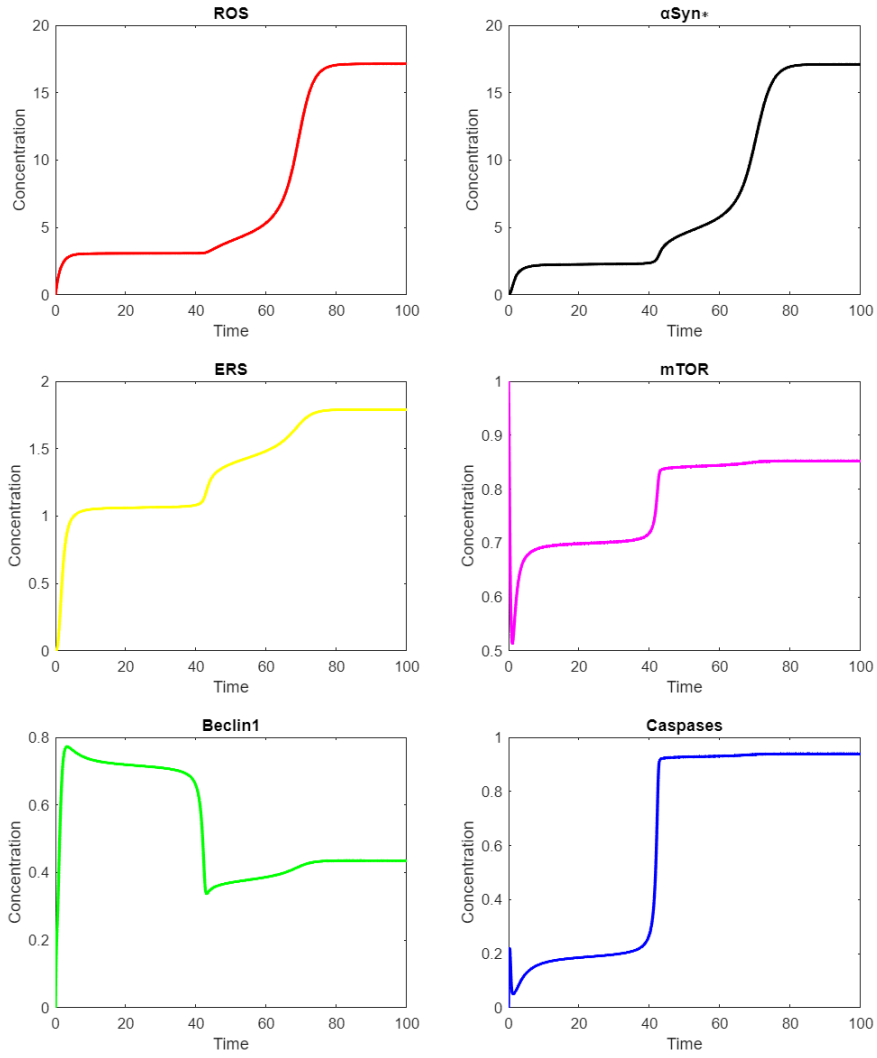

Figure 4: Outputs given own code 'odefun.m'.

As it can be seen, the outputs are quite similar between both methods one using a numerical solution with the Euler method (authors code), and the other using MATLAB's 'ode45' solver for solving ordinary differential equations (ODEs) as taught in class.

- **Euler Method Implementation**

The authors method uses a simple numerical solution approach, the Euler method. This will solve the ODEs system numerically, being a straightforward numerical integration technique that updates the state variables at each time step using simple difference equations.

The code includes functions for each component (ROS, αSyn, ERS, mTOR, Beclin1, and Caspases), being time evolution simulated using a `for` loop. The system state is updated at each time step based on the defined functions and parameters.

At last results are then plotted for each component separately using the `plot` function.

- **'ode45' Solver Implementation**

Our method uses the `ode45` solver, a built-in MATLAB function for solving ODEs. The ODEs system is defined in a separate function ('odefun.'), which takes care of the differential equations and parameters.

The ODE system is defined in the `odefun.m` function, which is passed to the `ode45` solver along with the time span and initial conditions. Then, the solver internally handles the numerical integration using more sophisticated algorithms than the Euler method.

At last, results are obtained as time points and concentrations, which are then plotted for each component separately.

- **Comparison**

The `ode45` solver generally provides more accurate results compared to the Euler method. `ode45` adapts the time step dynamically to capture rapid changes and avoids numerical instability issues.

Regarding implementation, the Euler method is simpler to implement manually, making it suitable for fast simulations. However, the `ode45` solver, is easier to use and requires less manual intervention. It is preferred for complex and real-world applications.

In addition, The Euler method may require a smaller time step to achieve accuracy, leading to longer computation times, while the `ode45` solver optimizes the time step adaptively, resulting in more efficient computations for many ODE systems.

Finally, the `ode45` is more robust for a wide range of ODE systems, handling stiff equations and various numerical challenges. The Euler method may become unstable for stiff ODEs or require a very small time step.

4.2. Bifurcation Diagrams and Tri-stability analysis through XPP-AUTO.

In order to explore the tri-stability analysis of the system through bifurcation diagrams the XPP-AUTO application is used as recommendation of the authors. They expressed the need to use a more robust approach than Matlab due to the difficulty of the ODE system, as they believe impossible to perform this type of task using the code we learn in class.

XPP AUTO is a software tool designed for the analysis and simulation of dynamical systems described by ODEs. Developed by Bard Ermentrout is widely used in the fields of mathematical biology, physics, and other scientific disciplines to study the behaviour of complex systems.

Key insights of XPP AUTO	
Dynamic Systems	XPP AUTO is primarily used for modeling and analyzing systems described by ordinary differential equations (ODEs). These systems often represent the time evolution of variables in various scientific and engineering applications.
Equation Definition	Users define their ODE systems using a simple text-based script. The script includes equations that describe the relationships between variables and their rates of change over time. For this project the document is called **'complex'**.
Bifurcation Analysis	It is particularly known for its capability to perform bifurcation analysis. Bifurcations are critical points where the behavior of a dynamical system changes qualitatively. XPP AUTO can identify bifurcation points and analyze the stability of solutions near these points.
Automated Continuation	One of the notable features of XPP AUTO is its ability to perform automated continuation. This involves systematically varying system parameters and automatically tracking how

	solutions change as these parameters are modified. This is especially useful for exploring the parameter space of a system.
Graphical User Interface	It comes with a graphical user interface that allows users to interact with the software more intuitively. It provides tools for setting up simulations, visualizing solutions, and exploring bifurcation diagrams.
Visualization and Plotting	The software includes visualization tools for plotting time series, phase portraits, and bifurcation diagrams. This makes it easier for users to interpret and analyze the behaviour of their dynamical systems.
Stability Analysis	It can perform stability analysis to determine the stability of fixed points or periodic orbits in a dynamical system. This is crucial for understanding the long-term behaviour of the system.
Extensibility	XPP AUTO allows users to define additional functions or events within their scripts, providing flexibility for modelling a wide range of systems with different characteristics.
Applications	It has been applied to a variety of fields, including neuroscience (neuronal dynamics), ecology, chemistry, and physics. It is used by researchers and scientists to gain insights into the behaviour of complex systems.

Below a figure of the interface can be seen, as well as some instructions for its download in reference [3].

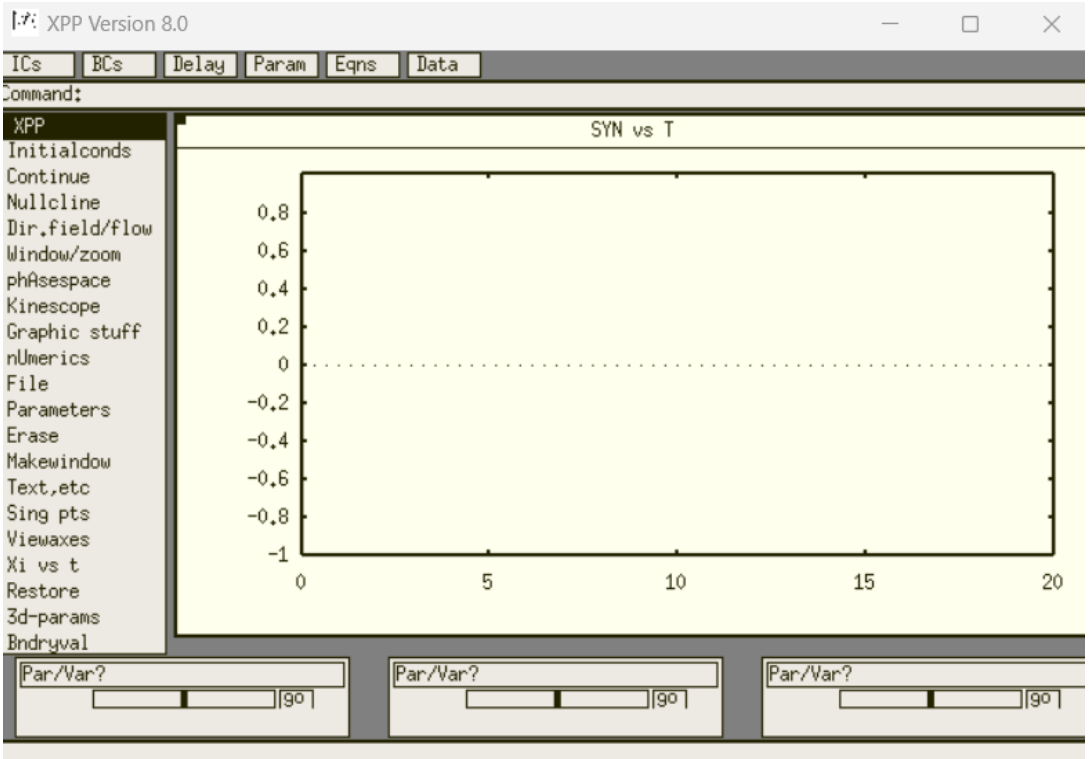

Figure 5: XPP-AUTO interface.

This tool allowed, for the specific task to be faced, enabled the visualization bifurcation diagrams in relation to the three stressors S1, S2, and S3. Tri-stability, a highlighted phenomenon in the article, has been analysed in detail. We will elaborate, with the use of XPP-AUTO, a specialized application for the analysis of dynamic systems, through the bifurcation diagram of the αSyn, Caspases and Beclin1 concentrations with respect to the three stressors. Thus, what we obtain is shown below:

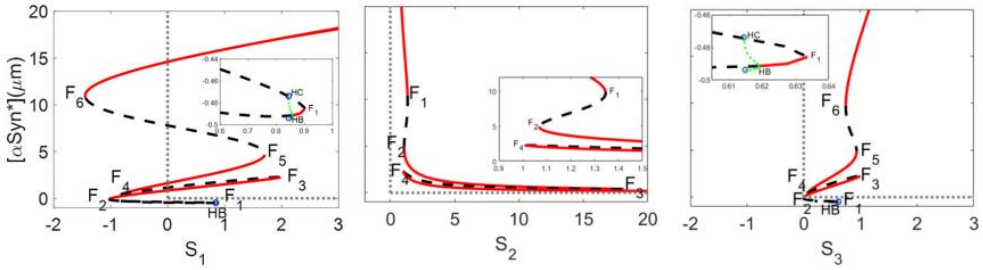

Figure 6: Bifurcation Diagram of αSyn concentration with respect the three stressors.

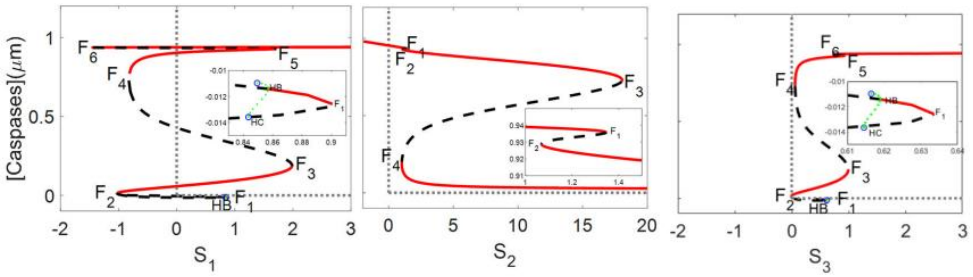

Figure 7: Bifurcation Diagram of Caspases concentration with respect the three stressors.

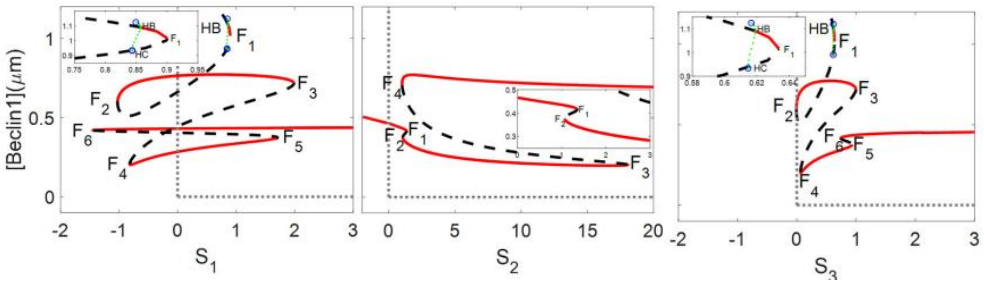

Figure 8: Bifurcation Diagram of Beclin1 concentration with respect the three stressors.

As we run out of space, all the documentation regarding XPP-AUTO implementation is presented in the references, with some video tutorials or documents explaining how it is used.

5. References.

[1] Yang B, Yang Z, Hao L. Dynamics of a model for the degradation mechanism of aggregated α-synuclein in Parkinson's disease. Front Comput Neurosci. 2023 Apr 13;17:1068150. doi: 10.3389/fncom.2023.1068150. PMID: 37122994; PMCID: PMC10133481.

[2] Yang B, Yang Z, Liu H, Qi H. Dynamic modelling and tristability analysis of misfolded α-synuclein degraded via autophagy in Parkinson's disease. Biosystems. 2023 Nov;233:105036. doi: 10.1016/j.biosystems.2023.105036. Epub 2023 Sep 17. PMID: 37726073.

[3] XPP/XPPAUT homepage. (s. f.). https://sites.pitt.edu/~phase/bard/bardware/xpp/xpp.html

[4] Marc R. Roussel (2004). Bifurcation Analysis with AUTO. https://people.uleth.ca/~roussel/nld/bifurc_analysis.pdf

[5] Chong, K. H. (2021). Tutorial for XPP AUTO to draw bifurcation diagram from periodic oscillations. ResearchGate. https://doi.org/10.13140/RG.2.2.31454.97607

[6] Angela Peace (2015). Tutorial on XPPAUT: Numerical Bifurcation Diagrams for ODEs. https://www.math.ttu.edu/~anpeace/files/XPPAUTOTutorial.pdf

[7] WR Holmes, May Anne Mata, Leah Edelstein-Keshet (2014). Local Perturbation Analysis (LPA) Tutorial using XPP. https://personal.math.ubc.ca/~keshet/Papers/LPA_BJTools_Supp1.pdf

[8] Bard Ermentrout (2012). XPPAUT5.41 – the differential equations tool.

[9] Eric Cytrynbaum. (2020, 3 noviembre). *An Introduction to XPPAUT - Part 1* [Vídeo]. YouTube. https://www.youtube.com/watch?v=tjLB3JDEXGs

[10] Eric Cytrynbaum. (2020b, noviembre 3). *An Introduction to XPPAUT - Part 2* [Vídeo]. YouTube. https://www.youtube.com/watch?v=SQZGlJUsKTg

[11] Syahirah Saini. (2017, 10 octubre). *XPPAUT download tutorial and how to use* [Vídeo]. YouTube. https://www.youtube.com/watch?v=45qdm_Tnqs4

[12] Eric Cytrynbaum. (2020c, noviembre 3). *Use XPPAUT to create a bifurcation diagram with periodic solutions for a substrate-depletion model* [Vídeo]. YouTube. https://www.youtube.com/watch?v=DzjIs3ry40o

[13] Vahab Youssof Zadeh. (2015, 30 junio). *Bifurcation diagram of Hodgkin-Huxley model using XPPAUT* [Vídeo]. YouTube. https://www.youtube.com/watch?v=Grr7N6FAAr8

[14] *Vahab* Youssof Zadeh. (2015b, julio 10). *Bifurcation Diagram of Jansen-RIT (1995) model using XPPAUT* [Vídeo]. YouTube. https://www.youtube.com/watch?v=JcqSsPzppp8

[15] Nottingham University. School of Mathematical Science. XPP Tutorial. https://www.maths.nottingham.ac.uk/plp/pmzsc/neurodynamics/XPPTutorial.pdf